QUANTUM OPTICS

Compressibility and the equation of state of an optical quantum gas in a box

Erik Busley, Leon Espert Miranda, Andreas Redmann, Christian Kurtscheid, Kirankumar Karkihalli Umesh, Frank Vewinger, Martin Weitz, Julian Schmitt*

The compressibility of a medium, quantifying its response to mechanical perturbations, is a fundamental property determined by the equation of state. For gases of material particles, studies of the mechanical response are well established, in fields from classical thermodynamics to cold atomic quantum gases. We demonstrate a measurement of the compressibility of a two-dimensional quantum gas of light in a box potential and obtain the equation of state for the optical medium. The experiment was carried out in a nanostructured dye-filled optical microcavity. We observed signatures of Bose-Einstein condensation at high phase-space densities in the finite-size system. Upon entering the quantum degenerate regime, the measured density response to an external force sharply increases, hinting at the peculiar prediction of an infinite compressibility of the deeply degenerate Bose gas.

Quantum gases of atoms, exciton-polaritons, and photons provide a test bed for many-body physics under both in- and out-of-equilibrium settings (*1*–*3*). Experimental control over dimensionality, potential energy landscapes, or the coupling to reservoirs offers wide possibilities to explore different phases of matter. For cold atomic gases, thermodynamic susceptibilities and transport properties have been extracted from density measurements (*4*–*9*) and have proven to be direct manifestations of the equation of state (EOS). In general, the EOS of a material—for example, its pressure-volume relation—describes both the thermodynamic state of a system under a given set of physical conditions as well as its response to perturbations as mechanical compression. Experimental investigations of the EOS in quantum gases constitute a tool for the characterization of phases and the identification of phase transitions, enabling important tests of physical models in a wide range of systems, from the ideal gas to superfluids and the interior of stars.

Quantum gases of light have so far been experimentally realized in low-dimensional settings, mostly two-dimensional (2D) systems (*3*). Thermalized photon gases with nonvanishing chemical potential μ as well as Bose-Einstein condensation (BEC) have been demonstrated in dye-filled optical microcavities at harmonic confinement (*10*–*12*), including measurements of density-insensitive thermodynamic quantities (*13*). By contrast, the isothermal compressibility $\kappa_T = n^{-2}(\partial n/\partial \mu)_T$ at temperature T depends on the (local) particle density n in the gas; for a systematic study, it thus is desirable to avoid spatially inhomogeneous density distributions inherent to harmonically trapped gases and instead prepare uniform samples, in which applying a spatially uniform force directly allows one to compress the gas and probe κ_T.

BEC does not occur in the infinite 2D homogeneous Bose gas given that thermal fluctuations at finite temperatures destroy long-range order (*14*). Although interactions nevertheless stabilize a superfluid through the Berezinskii-Kosterlitz-Thouless (BKT) mechanism, the infinite 2D ideal gas is doomed to remain quantum degenerate without forming a condensate. For a finite-sized homogeneous gas in a box, however, condensation is expected to be possible if the correlation length exceeds the system size at large phase-space densities (*15*). In ultracold atoms, the crossover between saturation-driven BEC and interaction-driven BKT superfluidity has been investigated in 2D harmonically trapped Bose gases by tuning the interactions using a Feshbach resonance (*16*), whereas studies of homogeneous gases in box potentials have focused on the interacting regime (*17*–*19*). In uniform gases of exciton-polaritons (*20*), on the other hand, the observation of BEC is hampered by reservoir-induced interactions and nonequilibrium effects. Up to now, the compressibility and the EOS have not been determined for optical quantum gases.

We examined a 2D quantum gas of photons in a box potential. In the finite-size homogeneous system, we observed BEC, as evidenced from the measured position and momentum distributions. In subsequent experiments, a mechanical force was exerted onto the photon gas prepared in a regime around the phase transition. By studying the density response to minute forces, we measured both the bulk isothermal compressibility and the EOS of the optical quantum gas.

Our homogeneous 2D photon gases were prepared in a nanostructured optical microcavity filled with a liquid dye solution (Fig. 1A) (*21*). The photons in the short cavity with mirror spacing on the order of the optical wavelength form a 2D gas of particles with an effective mass m, which are described by their transverse momentum $k = \sqrt{k_x^2 + k_y^2}$. To spatially confine the unbound plane-wave states of a 2D homogeneous system, we implemented a box potential of size L as a container for the photons. The box potential was realized by using a nanostructuring technique (*21*, *22*), which imprints a position-dependent static surface elevation onto one of the cavity mirrors. The locally reduced cavity length results in a repulsive potential. Thermalization of the photon gas to room temperature was achieved with absorption and reemission processes on the dye molecules (*10*). An exemplary density distribution of a trapped gas is shown in Fig. 1B, recorded by imaging the cavity emission, and optical frequency spectra over the trapped range $V_0/h \sim 2\pi \times 9$ THz above the cavity low-frequency cutoff $\nu_c = mc^2/(2\pi\hbar)$ are given in Fig. 1C, where $\hbar$ is the reduced Planck's constant and c is the speed of light,

Institut für Angewandte Physik, Universität Bonn, Wegelerstraße 8, 53115 Bonn, Germany.
*Corresponding author. Email: schmitt@iap.uni-bonn.de

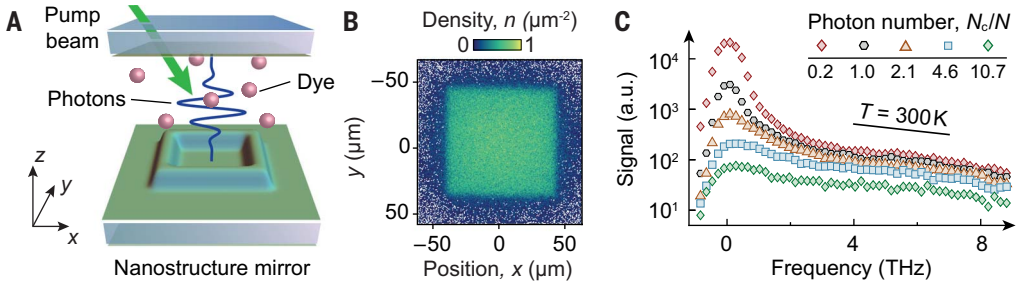

Fig. 1. Trapping a homogeneous 2D photon gas. (**A**) A spatially structured microcavity filled with dye molecules confines and thermalizes the uniform photon gas. The locally elevated surface of one of the cavity mirrors realizes a repulsive box potential. (**B**) Example surface density of a uniform photon gas in a square box with L = 80 μm. (**C**) Spectral distributions of the cavity emission exhibit an exponential decay that is consistent with $T \approx 300$ K, indicating a thermal equilibrium photon gas. The population in the low-frequency modes is enhanced as N_c/N approaches unity.

for different total particle numbers N. All spectra show an exponential decay of the population in the high-frequency states that is consistent with $k_B/(2\pi h) \times 300$ K, with Boltzmann's constant k_B, which we attribute as evidence for the gas to be thermalized. Moreover, the population in the lowest-lying states was enhanced as we increased N beyond a critical value N_c, which signals the emergence of a low-entropy phase.

We explored the quantum degenerate behavior in the finite-size homogeneous system. Surface densities in the box for different N are shown in Fig. 2A. Below the critical photon number N_c, the bulk density is uniform as for a normal gas, whereas above N_c, we observed a macroscopic occupation of the ground state $|\psi_{1,1}(x,y)|^2 = 4L^{-2}\cos^2(\pi x/L)\cos^2(\pi y/L)$, with $|x|, |y| \le L/2$; the qualitative change is evident from the line profiles. The corresponding momentum distributions below N_c in Fig. 2A resemble a Maxwell-Boltzmann distribution $f(k) \propto \exp(-k^2/\sigma_k^2)$, with $\sigma_k = \sqrt{2mk_BT}/\hbar$; for our data, $\sigma_k = 2.4(1)\,\mu m^{-1}$ gives $T = 295(33)$ K (where numbers in parentheses indicate errors calculated from the uncertainties of the fit parameters). Upon increasing the photon number, the population at small k is enhanced and ultimately dominated by a strongly occupied ground state at $k = 0$, the condensate. For large k, we observed signatures of both microscope aperture and finite trap depth (*21*). A closer inspection in x and k space (Fig. 2A, inset) confirms that the ground state is Heisenberg-limited with an uncertainty product $\Delta x \Delta k = 0.7(1)$, which is in agreement with theory $\Delta x \Delta k = \sqrt{\pi^2/12 - 1/2} \sim 0.6$.

To quantify the transition point, we studied the normalized spatial central density n_0L^2/N as a function of the particle number. The transition at $N_c = 3.5(4) \times 10^3$ is shown in Fig. 2B; the limiting cases $n_0L^2/N = 1$ for small N and $n_0L^2/N = 4$ for large N are well understood to arise from the uniform normal gas and inhomogeneous condensate density with N/L^2 and $4N/L^2$, respectively, at the center. The critical particle number scales with the predicted $N_c \propto (L/\lambda)^2\log(L/\lambda)$ (Fig. 2C), where $\lambda = 2\sqrt{\pi}/\sigma_k \sim 1.47\,\mu m$ denotes the thermal wavelength. The logarithmic scaling of the critical phase-space density $\mathcal{D}_c$ shown in Fig. 2C, inset, is understood from the dependence of the coherence length reaching the system size (*15*, *21*). At the largest investigated box sizes, we have $\mathcal{D}_c = N_c(\lambda/L)^2 = 6.3(8)$. For interacting 2D gases characterized by an interaction strength $\tilde{g}$ and realized in ultracold atoms (*6*, *7*, *15*–*17*, *19*), the BKT phase transition to a superfluid usually occurs before BEC; for example, for homogeneous gases, $\mathcal{D}_{c,BKT} = \log(380/\tilde{g}) \sim 6.5$ for $\tilde{g} = 0.6$ (*19*). Quite distinctly, for photon gases in dye microcavities, self-interactions with $\tilde{g} \le 10^{-6}$ (*23*) imply a much larger $\mathcal{D}_{c,BKT} \ge 20$, and accordingly, both phases are expected to be well separated.

We identified the BEC-like nature of the phase transition by extracting the ground and excited state populations N_0 and N_{exc}, respectively, from the momentum space distributions as a function of the total particle number N. The visible saturation of the normal part is shown in Fig. 3A, which indicates that interaction effects are very small (*24*); in particular, the saturation gives evidence that in our homogeneous finite-size system, BEC is prevalent instead of BKT. This interpretation is supported by the deduced caloric properties of the gas (Fig. 3B), which closely follow the ideal Bose gas prediction. For the internal energy $U = \langle E\rangle N_c/N^2 k_BT$, where $\langle E\rangle$ denotes the average transverse energy, we observed a crossover from a quadratic to a linear scaling in the condensed and normal phase, respectively, as a function of N_c/N. Correspondingly, its derivative $\partial U/\partial(N_c/N)$ is a smooth function, highlighting that the heat capacities in the normal and condensed phases are linked without any discontinuities (*8*, *13*). In the normal-gas phase, each particle can accommodate only $\approx 0.5k_BT$ of thermal energy, as well understood from the finite trap depth (*21*).

To determine the isothermal compressibility $\kappa_T = n^{-2}(\partial n/\partial\mu)_T$ of the optical quantum gas, we exerted a force onto the photons by tilting one of the cavity mirrors, which superimposes a linear potential $U(x) = U_0x/L$ to

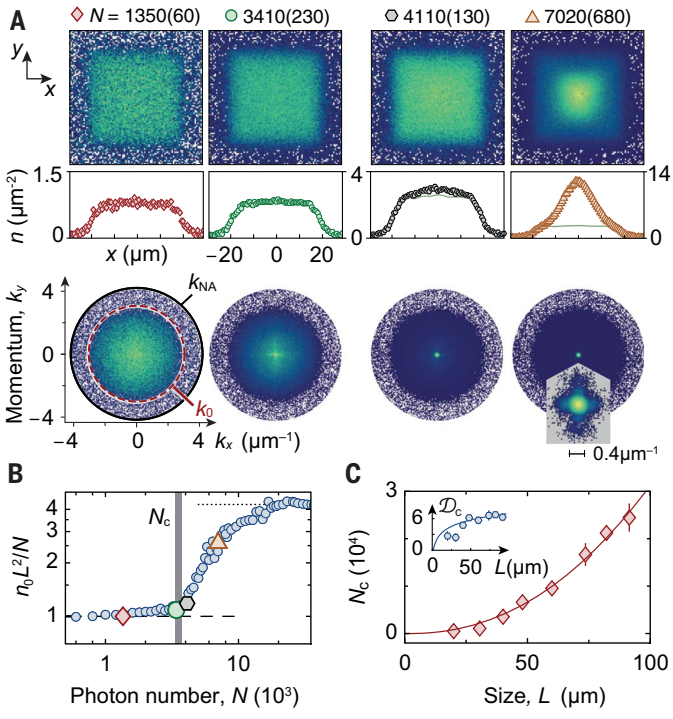

Fig. 2. Bose-Einstein condensation of photons in a box. (**A**) (Top) Density distributions, (middle) line profiles, and (bottom) momentum-space distributions (k_0 denotes the trap limit, k_{NA} denotes the imaging limit) as N is increased beyond $N_c = 3.5(4) \times 10^3$. Below N_c, the flat-top density and Gaussian k space distribution resemble a thermal gas in the normal phase. Above N_c, the ground state becomes massively populated and deforms the cloud, which is more directly observed in momentum space. (**B**) Normalized central spatial density versus N, starting from $n_0L^2/N = 1$ in the normal phase and approaching the expected value of 4 when the ground state dominates [symbols are as in (A)]. (**C**) N_c and (inset) $\mathcal{D}_c = N_c(\lambda/L)^2$, extracted from data as in (B), exhibit the predicted scaling (line) with the box size.

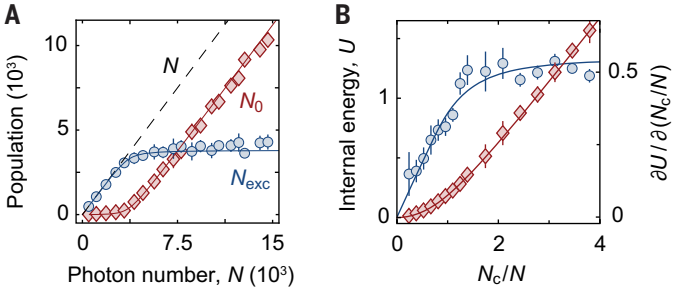

Fig. 3. Saturation and caloric properties. (**A**) Population in the ground (red) and excited states (blue), N_0 and N_{exc}, respectively, extracted from k space distributions (as in Fig. 2A, bottom) versus photon number N. At large N, the visible saturation of the normal part N_{exc} indicates that the phase transition is BEC-like. (**B**) Normalized internal energy (red), showing a crossover from quadratic (condensed gas, $N_c/N < 1$) to linear (normal, $N_c/N \gg 1$) scaling, and the derivative (blue), which reflects the specific heat per particle, versus N_c/N. In the normal phase, the latter reaches a value near 0.5, which is understood from the finite trap depth V_0, and is below the value of 1 expected for $V_0 \to \infty$. Solid lines are finite-size theory.

the box, and measured the density response. The displaced center of mass $\langle x \rangle$ (Fig. 4A, y axis) is shown in Fig. 4A as a function of the tilt U_0. In local density approximation (LDA), with chemical potential $\mu(x) = \mu_0 - U(x)$, the center of mass to first order relates to the compressibility, following $\langle x \rangle / L = -\kappa_T n U_0 / 12$ (*5*, *21*, *25*). For small U_0, the data in Fig. 4A confirms the linear behavior and shows an enhancement of the density response when going from the normal to the condensed phase. The visible saturation for large U_0 is caused by the finite box size, which limits the displacement.

The compressibility is shown in Fig. 4B, extracted from a linear fit of the region near $U_0 = 0$ (Fig. 4A), along with theory for the infinite and finite system. Below the critical density for condensation $N_c/L^2 \sim 2.6\ \mu m^{-2}$, the photon distribution is spatially homogeneous, as visible in Fig. 2, A and B. For these densities, LDA can be applied (*25*) to extract κ_T by using data with small tilts ($U_0 \lesssim \mu$), even in the case of very small interactions (*21*). In the condensed phase, however, the LDA ceases to be valid, and the corresponding region in Fig. 4B is shaded in gray. Within the region of validity, the compressibility compares well with theory. At densities $n \gtrsim 1\ \mu m^{-2}$, we observed a sharp increase of the compressibility; the onset is in good agreement with the prediction for an infinite noninteracting system (Fig. 4B, dashed line) (*21*). The corresponding function $\kappa_T = [\exp(n\lambda^2) - 1]/(k_B T n^2 \lambda^2)$ exhibits a minimum at $n \simeq 1.59/\lambda^2 \sim 0.74\ \mu m^{-2}$, which is close to the measured value of $0.79(5)\ \mu m^{-2}$. It is well understood that as the thermal wave packets spatially overlap, the classically expected decrease in compressibility with density (it is harder to compress a dense gas than a dilute one) is replaced with a compressibility increase that stems from the quantum-statistical occupation of low-lying energy levels, reducing the energy cost for compression as compared with that of the classical gas case. In the extreme high-density limit of an infinite-size deeply degenerate gas, bosons can be added to the system at essentially vanishing energy cost, meaning that $(\partial\mu/\partial n)_T$ gradually approaches zero as $\mu \to 0$, so that the compressibility takes arbitrarily large values.

Last, we studied the EOS $n = f(\mu, T)$ of the photon gas. The variation of the density n as a function of the chemical potential μ is shown in Fig. 4C, as determined from combining recorded density profiles of the gas in a tilted box at different N; an exemplary density deviation from the unperturbed case and the corresponding line profile $n(x)$ are given in Fig. 4C, insets. As above, the conversion from position to chemical potential relies on the potential gradient $U_0/L \approx k_B 0.6\ \mathrm{K}\,\mu m^{-1}$, which acts as a calibrated differential energy scale $d\mu = U_0/L\, dx$. Our data exhibit a larger slope than the EOS of the infinite 2D Bose gas, $n(\mu) = -\lambda^{-2}\log[1 - \exp(\mu/k_B T)]$ (Fig. 4C, dashed line) owing to the finite trap depth, as we confirmed with numerical calculations (*21*). Except for the condensed regime, in which LDA is invalid, our method reliably extracts the EOS of a quantum gas of light.

We have demonstrated a measurement of the compressibility of an optical quantum gas and determined its EOS. The experiment was carried out by using a 2D photon gas inside a box potential, both below and above the phase transition to a BEC. Compression of optical gases may have direct consequences for thermodynamic machines with light as a work medium (*26*). An additional perspective is the exploration of sound (*17*–*20*). The required dynamic manipulation of optical quantum gases is feasible through, for example, electro-optic trap modulation or spatiotemporally resolved pumping of the dye reservoir (*27*). Beyond ideal gas theory, a nonvanishing healing length can be achieved by either adding Kerr media or exploiting the weakly dissipative nature of photon condensates (*28*). The demonstrated homogeneous quantum gas of light in a box opens new possibilities for studies of universal phenomena in two dimensions, including critical behavior (*29*) and the nonequilibrium Kardar-Parisi-Zhang phase (*30*).

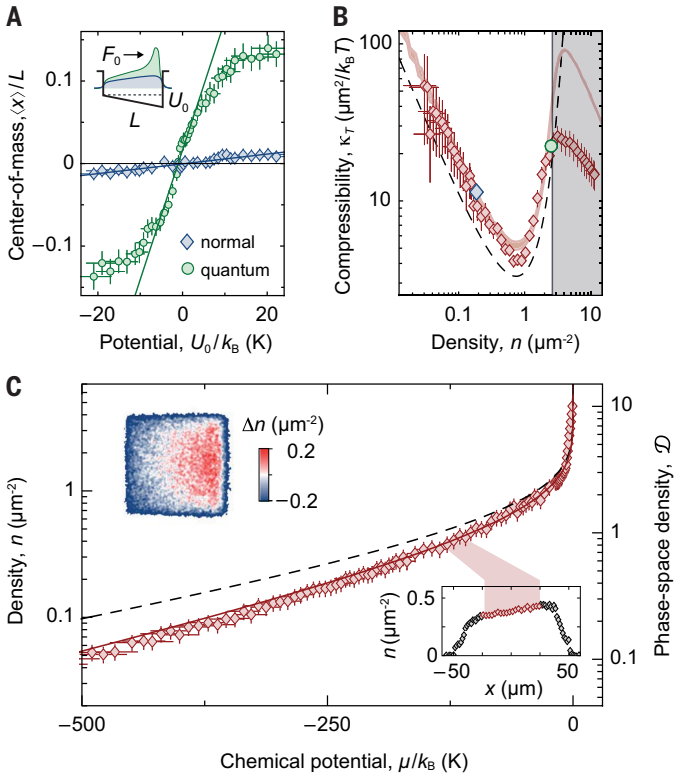

Fig. 4. Compressibility and EOS. (**A**) A linear potential realizes a force $F_0 = U_0/L$ that (inset) compresses the photon gas. Depending on its normal (blue) or quantum degenerate (green) state, the gas shows a different center-of-mass response, fitted in the linear response region (lines). (**B**) The compressibility κ_T decreases with density $n = N/L^2$, until above $n \sim 0.8\ \mu m^{-2}$ quantum degeneracy sets in and the Bose gas becomes highly compressible as a consequence of the gradually vanishing energy cost to increase the density. At $n \gtrsim 2.6\ \mu m^{-2}$ (shaded region), the κ_T extraction ceases to be valid; this range of validity has been confirmed numerically (*21*). For comparison, we show finite-size theory (red line; shading indicates uncertainty in V_0, which causes the vertical shift), where the kink at large densities is due to the finite box size, and the prediction for the infinite 2D Bose gas (dashed line). (**C**) From the density profiles, we extracted the EOS by combining data for different local chemical potentials (*21*). (Insets) Exemplary density deviation Δn from the case with $U_0 = 0$ and line profile. Lines show theory for finite-depth box (solid line) and infinite-system (dashed line).

REFERENCES AND NOTES

1. I. Bloch, J. Dalibard, W. Zwerger, *Rev. Mod. Phys.* **80**, 885–964 (2008).
2. S. Diehl *et al.*, *Nat. Phys.* **4**, 878–883 (2008).
3. I. Carusotto, C. Ciuti, *Rev. Mod. Phys.* **85**, 299–366 (2013).
4. N. Navon, S. Nascimbène, F. Chevy, C. Salomon, *Science* **328**, 729–732 (2010).
5. T. L. Ho, Q. Zhou, *Nat. Phys.* **6**, 131–134 (2010).
6. T. Yefsah, R. Desbuquois, L. Chomaz, K. J. Günter, J. Dalibard, *Phys. Rev. Lett.* **107**, 130401 (2011).
7. C. L. Hung, X. Zhang, N. Gemelke, C. Chin, *Nature* **470**, 236–239 (2011).
8. M. J. H. Ku, A. T. Sommer, L. W. Cheuk, M. W. Zwierlein, *Science* **335**, 563–567 (2012).
9. C. Mordini *et al.*, *Phys. Rev. Lett.* **125**, 150404 (2020).
10. J. Klaers, J. Schmitt, F. Vewinger, M. Weitz, *Nature* **468**, 545–548 (2010).
11. J. Marelic, R. A. Nyman, *Phys. Rev. A* **91**, 033813 (2015).
12. S. Greveling, K. L. Perrier, D. van Oosten, *Phys. Rev. A* **98**, 013810 (2018).
13. T. Damm *et al.*, *Nat. Commun.* **7**, 11340 (2016).
14. N. D. Mermin, H. Wagner, *Phys. Rev. Lett.* **17**, 1133–1136 (1966).
15. Z. Hadzibabic, J. Dalibard, *Riv. Nuovo Cim.* **34**, 389–434 (2011).
16. R. J. Fletcher *et al.*, *Phys. Rev. Lett.* **114**, 255302 (2015).
17. J. L. Ville *et al.*, *Phys. Rev. Lett.* **121**, 145301 (2018).
18. M. Bohlen *et al.*, *Phys. Rev. Lett.* **124**, 240403 (2020).
19. P. Christodoulou *et al.*, *Nature* **594**, 191–194 (2021).

20. E. Estrecho *et al*., *Phys. Rev. Lett.* **126**, 075301 (2021).
21. Materials and methods are available as supplementary materials.
22. C. Kurtscheid *et al*., *EPL* **130**, 54001 (2020).
23. D. Dung *et al*., *Nat. Photonics* **11**, 565–569 (2017).
24. N. Tammuz *et al*., *Phys. Rev. Lett.* **106**, 230401 (2011).
25. L. Pitaevskii, S. Stringari, *Bose-Einstein Condensation and Superfluidity* (Oxford Univ. Press, 2016).
26. A. Ghosh, V. Mukherjee, W. Niedenzu, G. Kurizki, *Eur. Phys. J. Spec. Top.* **227**, 2043–2051 (2019).
27. J. Schmitt *et al*., *Phys. Rev. A* **92**, 011602 (2015).
28. V. N. Gladilin, M. Wouters, *Phys. Rev. Lett.* **125**, 215301 (2020).
29. P. Comaron *et al*., *Phys. Rev. Lett.* **121**, 095302 (2018).
30. A. Zamora, L. M. Sieberer, K. Dunnett, S. Diehl, M. H. Szymańska, *Phys. Rev. X* **7**, 041006 (2017).
31. E. Busley *et al*., Zenodo (2021); doi:10.5281/zenodo.5775757.

ACKNOWLEDGMENTS

We thank F. König, C. Wahl, and D. Dung for experimental assistance and D. Luitz, P. Christodoulou, Z. Hadzibabic, and R. Lopes for fruitful discussions. **Funding:** This work was supported by the DFG within SFB/TR 185 (277625399) and the Cluster of Excellence ML4Q (EXC 2004/1–390534769) and by the EU within the Quantum Flagship project PhoQuS (820392). J.S. acknowledges support from an ML4Q Independence grant. **Author contributions:** Conceived and designed the experiments and analyzed the data: E.B., L.E.M., and J.S. Contributed materials and analysis tools: E.B., L.E.M., A.R., C.K., K.K.U., M.W., and J.S. Performed the experiments: E.B. and L.E.M. Wrote the paper: F.V., M.W., and J.S. **Competing interests:** The authors declare that they have no competing interests. **Data and materials availability:** The data described in the manuscript are available in the Zenodo database (*31*).

SUPPLEMENTARY MATERIALS

science.org/doi/10.1126/science.abm2543
Supplementary Text
Figs. S1 to S6
References (*32*–*36*)

3 September 2021; accepted 20 December 2021
10.1126/science.abm2543

Compressibility and the equation of state of an optical quantum gas in a box

Erik BusleyLeon Espert MirandaAndreas RedmannChristian KurtscheidKirankumar Karkihalli UmeshFrank VewingerMartin WeitzJulian Schmitt

Science, 375 (6587),

Putting light under pressure

The equation of state of a material system describes the various phases of the material under a set of physical conditions (pressure, volume, temperature, etc.). The same is true for quantum materials, in which exotic quantum phases can emerge. Busley *et al*. examined the mechanical properties of a quantum gas of light (see the Perspective by Fletcher and Zwierlein). Using light confined to a two-dimensional cavity with a box potential, the authors measured the compressibility of a photon gas in a regime around the phase transition to quantum degeneracy and determined its equation of state. The results hint at the formation of a highly compressible Bose-Einstein condensate, and this work provides a platform with which to study exotic quantum phases at room temperature. —ISO